23rd AIAA/CEAS Aeroacoustics conference, 5–9 June 2017, Denver, CO, USA

Nonlinear Acoustics in a Viscothermal Boundary Layer over an Acoustic Lining

Owen D. Petrie * Edward J. Brambley †

Sound within aircraft engines can be 120dB–160dB, and may be amplified by 1000× within a visco-thermal boundary layer over an acoustic lining. This may be expected to trigger nonlinear effects within the fluid boundary layer (in addition to the well-known nonlinear effects within the holes of the lining). This paper presents a mathematical investigation into the effects of weak nonlinearity on the acoustics within a thin boundary layer in flow over an acoustic lining in a duct. The analysis combines the effects of sheared mean flow, viscosity, and nonlinearity into an effective impedance boundary condition. In certain cases, a surprisingly large acoustic streaming effect is also found that is not localized to the boundary layer but propagates well out into the interior of the duct.

I. Introduction

Acoustic liners are an essential part of civilian aircraft engines, enabling them to meet ever stricter noise requirements. Sound within aircraft engines is loud, potentially 120dB–160dB, pushing the validity of the usual assumption of linearised sound over a steady background flow. However, a thin visco-thermal boundary layer of thickness δ over an acoustic lining was recently predicted[1] to give an amplification by a factor of order $1/\delta$ to certain elements of the acoustic solution. Since typically $\delta = 10^{-3}$ for aeroengine intakes, even when the sound within the engine ducting may validly be considered linear, nonlinear effects would be expected within the boundary layers over acoustic linings. Experimental evidence also suggests nonlinearity becomes important at lower amplitudes than might otherwise be expected for flow over an acoustic lining[2]. Here, these effects are investigated by mathematically modelling weakly nonlinear acoustics in a visco-thermal boundary layer over an acoustic lining.

Acoustic linings are typically modelled as an array of Helmholtz resonators; the effect of the acoustic lining is reduced to an impedance boundary condition, which is a linear relation between the acoustic pressure $\mathrm{Re}\big(\tilde{p}\exp\{\mathrm{i}\omega t - \mathrm{i}kx - \mathrm{i}m\theta\}\big)$ and the acoustic normal velocity $\mathrm{Re}\big(\tilde{v}\exp\{\mathrm{i}\omega t - \mathrm{i}kx - \mathrm{i}m\theta\}\big)$ at the boundary, $\tilde{p} = Z\tilde{v}$, where Z is typically a function of the frequency ω. Singh & Rienstra[3] showed that nonlinearity is generally unimportant for frequencies away from the resonant frequencies of the resonators, but that near the resonant frequencies the impedance needs to be modified to include a nonlinear term due to the inertia of the fluid in the resonator necks.

Much of the work on acoustics in flow over acoustic linings uses the Myers[4] boundary condition, $\frac{\tilde{p}}{\tilde{v}} = Z_{\mathrm{eff}} = \frac{\omega Z}{\omega - Mk}$, where Z is the actual boundary impedance and Z_{eff} is the effective boundary impedance seen by the acoustics in the uniform base flow of Mach number M within the duct. This comes from matching the normal fluid displacement at the boundary, and is correct for thin boundary layers, either at high frequencies[1,5] or for inviscid fluid[6,7]. However, the Myers boundary condition implies an infinitely thin boundary layer at the lining, and not only do boundary layers need to be extremely thin for this to be accurate[6,7], but it also causes the Myers boundary condition to be ill-posed[8]. More recent work[9] gave a modified Myers boundary condition which accounted for the thin sheared boundary layer of the background flow, but still ignored the effect of viscosity. However, Renou & Aurégan[10] demonstrated that to correlate mathematical and numerical results with the results of experiments, the effect of viscosity within

*PhD student, DAMTP, University of Cambridge, Cambridge CB3 0WA, United Kingdom. AIAA student member.

†Associate Professor and Royal Society University Research Fellow, Mathematics Institute and WMG, University of Warwick, Coventry, CV4 7AL, United Kingdom. AIAA senior member.

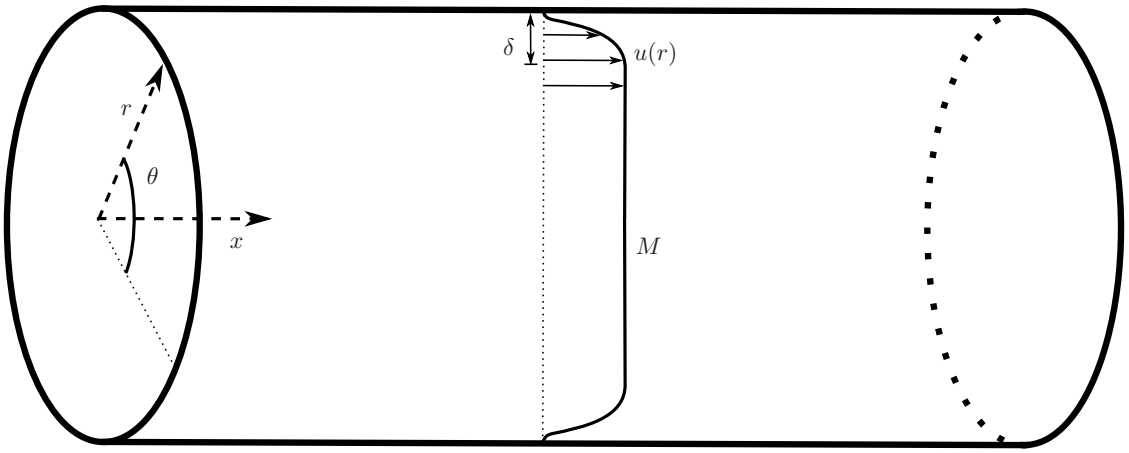

Figure 1: Diagram of the duct

Density	$\rho^* = \rho_0^* \rho$	Pressure	$p^* = c_0^{*2} \rho_0^* p$
Velocity	$\mathbf{u}^* = c_0^* \mathbf{u}$	Viscosity	$\mu = c_0^* l^* \rho_0^* \mu$
Distance	$x^* = l^* x$	Thermal Conductivity	$\kappa^* = c_0^* l^* \rho_0^* c_p^* \kappa$
Time	$t^* = l^*/c_0^* t$	Temperature	$T^* = c_0^{*2}/c_p^* T$

Table 1: Dimensional and Non-dimensional variables where $*$ denotes a dimensional variable, with lengthscale l^*, velocity c_0^*, density ρ_0^* and specific heat at constant pressure c_p^*.

the boundary layer must be included, while Khamis & Brambley[11,12] demonstrated that the effect of viscosity on the acoustics are of a comparable magnitude with the effect of shear, and thus both should be taken into account. Viscosity within the boundary layer was investigated by Aurégan *et al.*[5] for weak thin boundary layers, and by Brambley[1] for stronger thin boundary layers, while investigations of the boundary layer taking into account both base flow shear and viscosity have recently been performed by Khamis & Brambley[13,14]. This approach agrees most closely with results from solving the linearised Navier Stokes equations for the entire duct. The aim of all this work has been to derive a new boundary condition in terms of an effective impedance Z_{eff} as a function of the actual wall impedance Z. This is the impedance that an inviscid uniform flow would observe at the boundary given the effect of the viscous boundary layer. None of these studies have considered nonlinearity of the acoustics within the fluid.

In this paper the effect of nonlinearity is also considered. We restrict ourselves to the weakly nonlinear case $\varepsilon \ll \delta \ll 1$, where ε is the acoustic amplitude $\tilde{p}/p_0$ and δ is the boundary layer thickness.

II. Governing Equations

We consider the acoustics in a compressible viscous perfect gas inside a cylindrical duct, as depicted in figure 1. We non-dimensionalise all quantities as shown in table 1, giving the governing equations[15]

$$\frac{\partial \rho}{\partial t} + \nabla \cdot (\rho \mathbf{u}) = 0 \tag{1a}$$

$$\rho \frac{D\mathbf{u}}{Dt} = -\nabla p + \nabla \cdot \sigma \tag{1b}$$

$$\sigma_{ij} = \mu \left(\frac{\partial u_i}{\partial x_j} + \frac{\partial u_j}{\partial x_i} \right) + \left(\mu^B - \tfrac{2}{3}\mu \right) \delta_{ij} \nabla \cdot \mathbf{u} \tag{1c}$$

$$\rho \frac{DT}{Dt} = \frac{Dp}{Dt} + \nabla \cdot (\kappa \nabla T) + \sigma_{ij} \frac{\partial u_i}{\partial x_j} \tag{1d}$$

$$T = \frac{p}{(\gamma - 1)\rho} \tag{1e}$$

where $D/Dt = \partial/\partial t + \mathbf{u} \cdot \nabla$ and $\gamma = c_p^*/c_v^*$ is the ratio of specific heats. We assume that the viscosities and thermal conductivity depend linearly on the temperature and are independent of pressure (Prangsma,

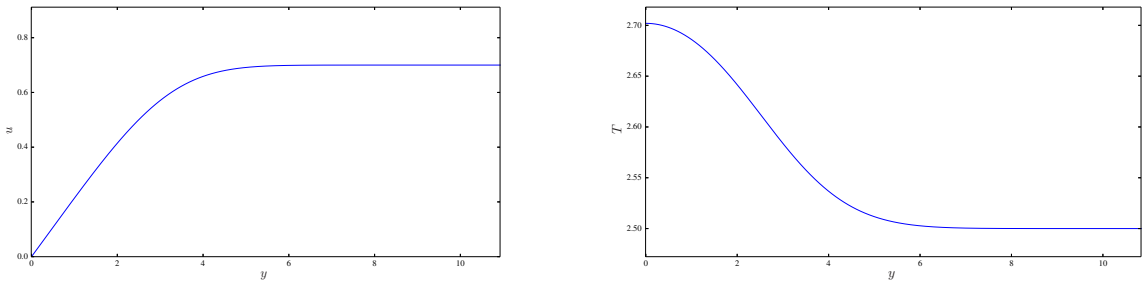

Figure 2: Boundary Layer Profile (u left, T right) for $M = 0.7$, $\mathrm{Pr} = 0.7$, $\xi = 1$ and $\delta = 10^{-3}$

Alberga & Beenakker)[16],

$$\mu = \frac{T}{T_0 \mathrm{Re}}, \quad \mu^B = \frac{T}{T_0 \mathrm{Re}} \frac{\mu_0^{B^*}}{\mu_0^*}, \quad \kappa = \frac{T}{T_0 \mathrm{Pr} \mathrm{Re}} \tag{2}$$

where $\mathrm{Re} = c_0^* l^* \rho_0^* / \mu_0^*$ is the Reynolds number based on the sound speed and $\mathrm{Pr} = \mu_0^* c_p^* / \kappa_0^*$ is the Prandtl number. In the duct we use cylindrical coordinates (r^*, θ, x^*) where l^* is now taken to be the radius of the duct, so that in non-dimensionalised variables the wall of the duct is at $r = 1$. We assume that the mean flow is uniform and time-independent and has a boundary layer thickness δ^*. We then take the reference values ρ_0^*, T_0^*, μ_0^*, $\mu_0^{B^*}$ and κ_0^* to be those of the uniform flow. This gives $T_0 = 1/(\gamma - 1)$ and $p_0 = 1/\gamma$. The non-dimensionalised uniform flow velocity $U_0 = M$ is the Mach number.

At the duct boundary $r^* = l^*$ we consider a steady thin boundary layer of thickness $\delta^* = l^* \delta$. The boundary layer is characterised by balancing viscous shear with inertia, so that inside the boundary layer we use the scalings

$$r = 1 - \delta y, \qquad \xi \delta^2 = 1/\mathrm{Re} \tag{3}$$

where $\xi \sim \mathcal{O}(1)$ is a parameter adjusting the relative strength of viscosity, and $\xi = 0$ gives an inviscid boundary layer. Any boundary layer profile could be used for what follows, provided it is independent of t and θ and is in thermal equilibrium with the boundary, $T_r(1) = 0$. For the results given here, a compressible Blasius boundary layer is used, as depicted in figure 2; for further details, see Ref. 1.

For a typical aircraft engine at sea level, $\rho_0^* \approx 1.225 \mathrm{kgm}^{-3}$, $c_0^* \approx 340 \mathrm{ms}^{-1}$, $\mu_0^* \approx 2 \times 10^{-5} \mathrm{Pa}$, $c_p^* \approx 10^3 \mathrm{m}^2 \mathrm{s}^{-2} \mathrm{K}$, $\gamma \approx 1.4$ and $l^* \approx 1\mathrm{m}$. This then gives the order of magnitude estimates $\mathrm{Re} \approx 10^7$, and hence $\delta \approx 10^{-3}$. For acoustic power between 120dB and 160dB, we find ε has an order of magnitude varying between 5×10^{-5} and 5×10^{-3}. For the subsequent weakly nonlinear approximation, we will require $\varepsilon \ll \delta$.

III. Small perturbations

We now consider small perturbations to the uniform flow of magnitude $\varepsilon \ll \delta$ that are the real part of terms with dependence $\exp\{\mathrm{i}(\omega t - kx - m\theta)\}$. We will write, for example, the total temperature as $T + \tilde{T}$, where $T(r)$ is the mean flow value and $\tilde{T}$ is the small harmonic perturbation.

Outside the boundary layer (i.e. within the duct away from the walls) we assume gradients are not large, so that the viscous terms, which are $\mathcal{O}(1/\mathrm{Re}) = \mathcal{O}(\delta^2)$ from (2), can be neglected at leading order. This means that at leading order we can treat the flow outside the boundary layer as inviscid with $\mathbf{u} = (M + \tilde{u}_O, \tilde{v}_O, \tilde{w}_O)$, $p = 1/\gamma + \tilde{p}_O$ and $T = 1/(\gamma - 1) + \tilde{T}_O$.

Inside the boundary layer, we rescale using (3), so that $r = 1 - \delta y$ and $\mathbf{u} = (u + \tilde{u}, -\delta \tilde{v}, \tilde{w})$. From Ref. 1 we know that for the leading order system to be well-posed we require $\tilde{u}$, $\tilde{v}$, $\tilde{\rho}$ and $\tilde{T}$ to be $\mathcal{O}(\varepsilon/\delta)$ and $\tilde{p}$

and $\tilde{w}$ to be $\mathcal{O}(\varepsilon)$ at leading order. This suggests we use the expansion:

$$\tilde{u} = \frac{\varepsilon}{\delta}\tilde{u}_1 + \frac{\varepsilon^2}{\delta^2}\tilde{u}_2 + \varepsilon\tilde{u}_3 \tag{4a}$$

$$\tilde{v} = \frac{\varepsilon}{\delta}\tilde{v}_1 + \frac{\varepsilon^2}{\delta^2}\tilde{v}_2 + \varepsilon\tilde{v}_3 \tag{4b}$$

$$\tilde{w} = \varepsilon\tilde{w}_1 + \frac{\varepsilon^2}{\delta}\tilde{w}_2 + \varepsilon\delta\tilde{w}_3 \tag{4c}$$

$$\tilde{T} = \frac{\varepsilon}{\delta}\tilde{T}_1 + \frac{\varepsilon^2}{\delta^2}\tilde{T}_2 + \varepsilon\tilde{T}_3 \tag{4d}$$

$$\tilde{p} = \varepsilon\tilde{p}_1 + \frac{\varepsilon^2}{\delta}\tilde{p}_2 + \varepsilon\delta\tilde{p}_3 \tag{4e}$$

where the quantities labelled '1' are the leading order (linear) perturbations, quantities labelled '2' are the first order nonlinear correction, and quantities labelled '3' are the first order in δ linear correction (i.e. the first terms to involve mean flow shear). We next expand the governing equations (1) to order $\mathcal{O}(\varepsilon^2)$ and $\mathcal{O}(\varepsilon\delta)$ to give linear system of ODEs for each of these quantities.

IV. Linear acoustics

In this section we describe the process for solving the governing equations (1) with the asymptotic expansion (4) for the leading order linear terms (quantities labelled '1'), reproducing the results of Ref. 1. A similar procedure can be used for the first order linear correction terms (quantities labelled '3'), as was done in Ref. 13. These equations will be used in section V to calculate the new nonlinear terms (quantities labelled '2').

Since the equations we are working with here are linear, we do not have to take the real parts of the complex exponentials when substituting for the perturbations, but may work instead directly with the complex exponentials, as is usual in acoustics.

A. Outer

At leading order the solution for the pressure in the centre of the duct is the standard result involving Bessel functions,

$$\tilde{p}_O = CJ_m(\alpha r) \qquad \text{where} \qquad \alpha^2 = (\omega - Mk)^2 - k^2, \tag{5}$$

and C is an arbitrary constant. The other quantities are then given in terms of $\tilde{p}_O$ by

$$\mathrm{i}(\omega - Mk)\tilde{u}_O - \mathrm{i}k\tilde{p}_O = 0, \tag{6a}$$

$$\mathrm{i}(\omega - Mk)\tilde{v}_O + \tilde{p}_{Or} = 0, \tag{6b}$$

$$\mathrm{i}(\omega - Mk)\tilde{w}_O - \mathrm{i}m\tilde{p}_O/r = 0, \tag{6c}$$

$$\tilde{T}_O = \tilde{p}_O. \tag{6d}$$

B. Inner

Inside the boundary layer, the expansion of the governing equations (1) at leading order gives

$$\mathcal{L}(\tilde{u}_1, \tilde{v}_1, T_1; \omega, k) = \left\{ \begin{array}{c} i(\omega - uk)\tilde{T}_1 + T_y\tilde{v}_1 - T\tilde{v}_{1y} + ikT\tilde{u}_1 \\ i(\omega - uk)\tilde{u}_1 + \tilde{v}_1 u_y - \xi(\gamma-1)^2 T(T\tilde{u}_{1y} + \tilde{T}_1 u_y)_y \\ i(\omega - uk)\tilde{T}_1 + \tilde{v}_1 T_y - \xi(\gamma-1)^2 T\left[\frac{1}{Pr}(\tilde{T}_1 T)_{yy} + \tilde{T}_1(u_y)^2 + 2Tu_y\tilde{u}_{1y}\right] \end{array} \right\} = \mathbf{0} \tag{7}$$

which is a system of linear homogeneous ODEs.

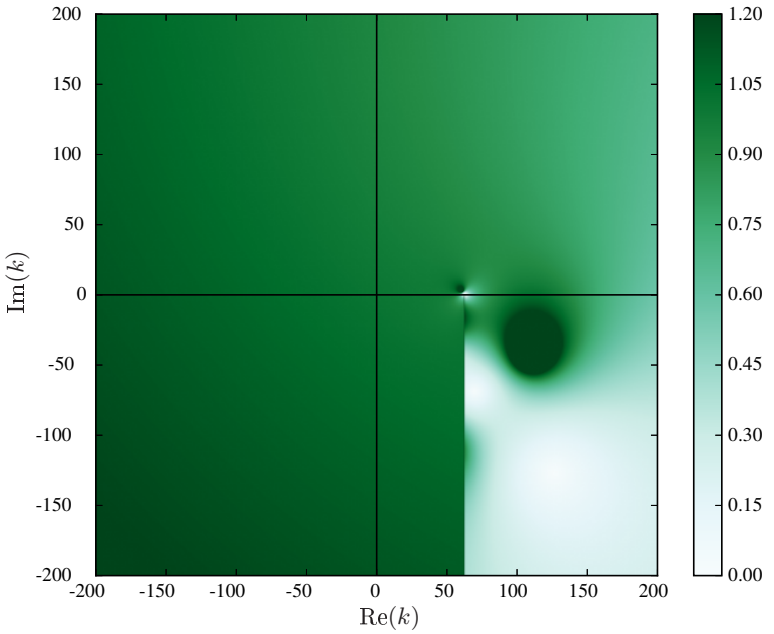

Figure 3: Surface plot of $|Z_{\text{eff}}/Z(1-\frac{Mk}{\omega})|$ in the k-plane for $\omega = 31$, $M = 0.5$, $\delta = 10^{-3}$, Pr $= 0.7$ and $\xi = 1$. The darker shades of green are where the Myers condition agrees fairly closely with the viscous asymptotics whereas the lighter shades are where the two schemes disagree.

C. Matching

The system of equations $\mathcal{L}$ is second order in $\tilde{u}$ and $\tilde{T}$, and (due to the scaling used, 4) we have that $\tilde{u}_1 = \tilde{T}_1 = 0$ at the wall. To get the second boundary condition we look outside the boundary layer, where the gradients of the mean flow quantities vanish and the mean flow quantities achieve their uniform flow values, so at $y = Y \gg 1$, the system decouples and becomes:

$$\mathcal{L}(\tilde{u}_1, \tilde{v}_1, T_1; \omega, k) = \left\{ \begin{array}{c} \eta_\infty^2 \tilde{T}_1 - \frac{1}{(\gamma-1)}\tilde{v}_{1y} + \frac{ik}{(\gamma-1)}\tilde{u}_1 \\ \eta_\infty^2 \tilde{u}_1 - \xi \tilde{u}_{1yy} \\ \eta_\infty^2 \tilde{T}_1 - \frac{\xi}{Pr}\tilde{T}_{1yy} \end{array} \right\} = \mathbf{0} \tag{8}$$

This can now be solved analytically, with only the decaying solutions kept so that we can match to our Outer solution in the centre of the duct. This allows the equations at Y to be reformulated to give first order equations such that only the decaying solutions are admitted:

$$\tilde{u}_{1y} + \eta_\infty \tilde{u}_1 = 0, \quad \tilde{v}_1 = \tilde{v}_{1\infty} - \frac{\eta_\infty(\gamma-1)\xi}{\sigma}\tilde{T}_1 - \frac{ik}{\eta_\infty}\tilde{u}_1, \quad \tilde{T}_{1y} + \sigma\eta_\infty \tilde{T}_1 = 0 \quad \text{at } y = Y$$

where $\eta_\infty^2 = i(\omega - Mk)/\xi$ and $\sigma^2 = Pr$. This gives the results of Brambley[1]; where the $\mathcal{O}(\varepsilon/\delta)$ amplification in the boundary layer does not propagate into the centre of the duct where the acoustics are $\mathcal{O}(\varepsilon)$. This is because both $\tilde{u}_1$ and $\tilde{T}_1$ decay to zero outside the boundary layer, while $-\delta\tilde{v}_{1\infty}$, which is $\mathcal{O}(\varepsilon)$, is matched to the outer. It should be noted that taking the decaying solution involves taking the square root of η_∞^2 which has positive real part. This leads to a branch cut in the complex k-plane, with the branch point at $k = \omega/M$ and the branch cut extending vertically downwards.

Figure 3 shows a plot of $|Z_{\text{eff}}/Z(1-\frac{Mk}{\omega})|$ in the k-plane for the leading order viscous asymptotics. This compares the effective impedance found to the impedance from the Myers boundary condition. The branch cut is clearly visible at $\text{Re}(k) = 62$ for $\text{Im}(k) < 0$.

For further details of this, including various asymptotic solutions of (7) in high- and low-frequency limits, the reader is referred to Ref. 1. The same procedure as given here may be used to calculate the first order linear correction terms (quantities labelled '3' above), and such an analysis is given in Ref. 13. We now turn our attention to the nonlinear correction terms.

V. Nonlinear acoustics

Having solved for the leading order linear terms, We now solve for the nonlinear correction terms (quantities labelled '2' in 4). Substituting the asymptotic ansatz (4) into the governing equations (1) and taking terms of order $\mathcal{O}(\varepsilon^2)$ results in a set of linear ODEs to solve for the nonlinear correction terms, forced by terms quadratic in the leading order linear solution. Since these forcing terms are nonlinear, we must take the real parts of the perturbed leading order quantities before multiplying. For example, the multiple of $\tilde{u}_1$ and $\mathrm{d}\tilde{v}_1/\mathrm{d}x$ is

$$\begin{aligned}\mathrm{Re}\big(\tilde{u}_1\exp\{\mathrm{i}\omega t-\mathrm{i}kx-\mathrm{i}m\theta\}\big)\,\mathrm{Re}\big(-\mathrm{i}k\tilde{v}_1\exp\{\mathrm{i}\omega t-\mathrm{i}kx-\mathrm{i}m\theta\}\big)\\ =\frac{1}{2}\mathrm{Re}\Big(-\mathrm{i}k\tilde{u}_1\tilde{v}_1\exp\{2\mathrm{i}\omega t-2\mathrm{i}kx-2\mathrm{i}m\theta\}+\mathrm{i}k^\star\tilde{u}_1\tilde{v}_1^\star\exp\{\mathrm{i}(\omega-\omega^\star)t-\mathrm{i}(k-k^\star)x\}\Big),\end{aligned}\tag{9}$$

where a star denotes the complex conjugate. This therefore results in two different modes: a mode of double the frequency and wavenumber of the leading order acoustics; and a 'zero' frequency mode that has the purely imaginary frequency $\omega-\omega^\star$ and wavenumber $k-k^\star$.

A. Inner

The system of equations to solve is now:

$$\mathcal{L}(\tilde{u}_2,\tilde{v}_2,\tilde{T}_2;\Omega,K)=\mathcal{Q}(\tilde{u}_1,\tilde{v}_1,\tilde{T}_1;\tilde{u}_1^\star,\tilde{v}_1^\star,\tilde{T}_1^\star;\omega,k)\tag{10}$$

where $\mathcal{L}$ is as given in (7), $\Omega=2\omega$, $K=2k$ and the $\star$ is ignored in the double frequency mode case, and $\Omega=\omega-\omega^\star$, $K=k-k^\star$ and the $\star$ means the complex conjugate in the 'zero' mode case. The forcing $\mathcal{Q}$ has the following form:

$$\mathcal{Q}=\left\{\begin{array}{c}\frac{T_y}{2T}(\tilde{T}_1\tilde{v}_1^\star)-\frac{1}{4}(\tilde{T}_1\tilde{v}_1^\star)_y+\frac{\tilde{T}_1\tilde{T}_1^\star}{4T}i(\Omega-uK)+\frac{1}{4}iK\tilde{u}_1\tilde{T}_1^\star\\ \frac{i(\omega-uk)}{4T}(\tilde{u}_1\tilde{T}_1^\star)+\frac{ik}{4}\tilde{u}_1\tilde{u}_1^\star+\frac{u_y}{4T}(\tilde{T}_1\tilde{v}_1^\star)-\frac{1}{4}(\tilde{v}_1\tilde{u}_{1y}^\star)+\frac{\xi(\gamma-1)^2T}{4}(\tilde{T}_1\tilde{u}_{1y}^\star)_y\\ \frac{ik}{4}(\tilde{u}_1^\star\tilde{T}_1)-\frac{1}{4}(\tilde{v}_1\tilde{T}_{1y}^\star)+\frac{i(\omega-uk)}{4T}\tilde{T}_1\tilde{T}_1^\star+\frac{T_y}{4T}(\tilde{T}_1\tilde{v}_1^\star)+\\ +\frac{\xi(\gamma-1)^2T}{4Pr}(\tilde{T}_1^\star\tilde{T}_{1y})_y+\frac{\xi(\gamma-1)^2T}{4}(T\tilde{u}_{1y}\tilde{u}_{1y}^\star+2u_y\tilde{T}_1\tilde{u}_{1y}^\star)\end{array}\right\}\tag{11}$$

Similarly to the linear case, when the extrapolation outside the boundary layer at $y=Y\gg1$ is carried out we get exponential terms $\propto\exp(\pm N_\infty y)$ where $N_\infty^2=i(\Omega-MK)/\xi$. The double frequency mode behaves similarly to the leading order acoustics. The branch cut for N_∞ is the same as for η_∞, and we can take the decaying solution and rewrite the equations to ensure only this solution is admitted. However for the 'zero' mode N_∞^2 is always real, and the resulting behaviour depends on the sign of N_∞^2. For downstream decaying modes, $N_\infty^2<0$, and both exponentials have purely imaginary argument and oscillate without decaying. In effect, this is because in this case the whole lower-half k-plane is the branch cut. This means that the $\mathcal{O}(\varepsilon^2/\delta^2)$ 'zero' frequency amplification will propagate into the centre of the duct. For upstream decaying modes, $N_\infty^2>0$, and the decaying solution may be taken similarly to the leading order case.

B. Interaction of multiple modes

We might also consider the nonlinear effect due to two different frequency leading order modes interacting. We now take the leading order acoustics as a superposition of two waves,

$$\tilde{u}_1=\mathrm{Re}\left(\tilde{u}_{1a}e^{i(\omega_at-k_ax-m_a\theta)}\right)+\mathrm{Re}\left(\tilde{u}_{1b}e^{i(\omega_bt-k_bx-m_b\theta)}\right),\tag{12}$$

We finally obtain two pairs of nonlinear self-interaction modes, as described above, as well as two cross-interaction modes. These cross-interactions modes will have the forms

$$\tilde{u}_{2+}=\mathrm{Re}\big(\tilde{u}_2e^{i[(\omega_a+\omega_b)t-(k_a+k_b)x-(m_a+m_b)\theta]}\big),\qquad\tilde{u}_{2-}=\mathrm{Re}\big(\tilde{u}_2e^{i[(\omega_a-\omega_b^\star)t-(k_a-k_b^\star)x-(m_a-m_b)\theta]}\big).\tag{13}$$

The system of equations we now have to solve are:

$$\mathcal{L}(\tilde{u}_{2+},\tilde{v}_{2+},\tilde{T}_{2+};\Omega,K)=\mathcal{Q}(\tilde{u}_{1a},\tilde{v}_{1a},\tilde{T}_{1a};\tilde{u}_{1b},\tilde{v}_{1b},\tilde{T}_{1b};\omega_a,k_a)+\mathcal{Q}(\tilde{u}_{1b},\tilde{v}_{1b},\tilde{T}_{1b};\tilde{u}_{1a},\tilde{v}_{1a},\tilde{T}_{1a};\omega_b,k_b) \quad (14)$$

with $\mathcal{Q}$ from (11), $\Omega=\omega_a+\omega_b$ and $K=k_a+k_b$, and

$$\mathcal{L}(\tilde{u}_{2-},\tilde{v}_{2-},\tilde{T}_{2-};\Omega,K)=\mathcal{Q}(\tilde{u}_{1a},\tilde{v}_{1a},\tilde{T}_{1a};\tilde{u}^\star_{1b},\tilde{v}^\star_{1b},\tilde{T}^\star_{1b};\omega_a,k_a)+\mathcal{Q}(\tilde{u}^\star_{1b},\tilde{v}^\star_{1b},\tilde{T}^\star_{1b};\tilde{u}_{1a},\tilde{v}_{1a},\tilde{T}_{1a};-\omega^\star_b,-k^\star_b)$$

with $\Omega=\omega_a-\omega^\star_b$ and $K=k_a-k^\star_b$.

The magnitude of the matching outer solution depends on N^2_∞ in the same way as the self-interaction modes. For N^2_∞ real and negative the outer solution is $\mathcal{O}(\varepsilon^2/\delta^2)$, and for all other values of N^2_∞ it is $\mathcal{O}(\varepsilon^2)$.

C. Outer

In the case $N^2_\infty>0$ (when the original mode decays in the upstream direction) the behaviour of the 'zero' mode outside the boundary layer is similar to the leading order mode, the amplification in the boundary layer decays and it matches to a $\mathcal{O}(\varepsilon^2)$ Outer solution which is given by a forced Bessel's equation:

$$\begin{aligned}\tilde{p}_{2rr}+\frac{1}{r}\tilde{p}_{2r}+A^2\tilde{p}_2-\frac{\mathcal{M}^2}{r^2}\tilde{p}_2=&\frac{(\gamma-1)\xi^2\eta^2_\infty N^2_\infty}{4}\tilde{p}^\star_1\tilde{T}_1-\frac{(\gamma-1)\xi^2N^4_\infty}{4}\tilde{p}^\star_1\tilde{T}_1\\
&-\frac{iK\xi N^2_\infty}{4}\tilde{p}^\star_1\tilde{u}_1+\frac{\xi N^2_\infty}{4}(\frac{\tilde{v}_1}{r}+\tilde{v}_{1r})\tilde{p}^\star_1+\frac{\xi N^2_\infty}{4}\tilde{v}_1\tilde{p}^\star_{1r}-\frac{i\mathcal{M}\xi N^2_\infty}{4r}\tilde{w}_1\tilde{p}^\star_1\\
&+\frac{iK}{4}[\xi\eta^2_\infty\tilde{p}^\star_1\tilde{u}_1-ik\tilde{u}^\star_1\tilde{u}_1+\tilde{v}^\star_1\tilde{u}_{1r}-\frac{im}{r}\tilde{w}^\star_1\tilde{u}_1]\\
&+\frac{1}{4r}[-\xi\eta^2_\infty\tilde{p}^\star_1\tilde{v}_1+ik\tilde{u}^\star_1\tilde{v}_1-\tilde{v}^\star_1\tilde{v}_{1r}+\frac{im}{r}\tilde{w}^\star_1\tilde{v}_1+\frac{1}{r}\tilde{w}^\star_1\tilde{w}_1]\\
&+\frac{1}{4}[-\xi\eta^2_\infty\tilde{p}^\star_1\tilde{v}_1+ik\tilde{u}^\star_1\tilde{v}_1-\tilde{v}^\star_1\tilde{v}_{1r}+\frac{im}{r}\tilde{w}^\star_1\tilde{v}_1+\frac{1}{r}\tilde{w}^\star_1\tilde{w}_1]_r\\
&+\frac{i\mathcal{M}}{4r}[-p^\star_1\eta^2_\infty\xi\tilde{w}_1+ik\tilde{u}^\star_1\tilde{w}_1-\tilde{v}^\star_1\tilde{w}_{1r}+\frac{im}{r}\tilde{w}^\star_1\tilde{w}_1-\frac{1}{r}\tilde{v}^\star_1\tilde{w}_1]+c.c.\end{aligned}$$

where $A^2=-\xi^2N^4_\infty-K^2=[\Omega-MK]^2-K^2$ and $\mathcal{M}=0$. This can be transformed to a forced Bessel's equation of order $\mathcal{M}$. For the double mode the equation for the outer is the same but with $\mathcal{M}=2m$.

D. Outer for self-interaction mode with $N^2_\infty<0$

In the case $N^2_\infty<0$, the extrapolation of the inner gives an oscillatory solution. This propagates into the rest of the duct and as the frequency of the oscillations is $\propto 1/\delta$, the gradients outside the boundary layer can no longer be assumed to be small and so the viscous terms cannot be ignored. However, an approximate solution to the outer equations may be found using the method of multiple scales. To do this we begin by defining variables y and Y such that $r=Y+\delta y$, so y is the rapidly varying variable and Y the slowly varying variable. We can then expand all quantities as $\tilde{u}_2=\frac{\varepsilon^2}{\delta^2}\tilde{u}_{O0}+\frac{\varepsilon^2}{\delta}\tilde{u}_{O1}+\varepsilon^2\tilde{u}_{O2}$ and expand the equations in powers of δ. At leading order ($\mathcal{O}(\varepsilon^2/\delta^2)$) this gives:

$$N^2_\infty\xi\tilde{u}_{O0}-\xi\tilde{u}_{O0yy}=0 \qquad \Rightarrow \qquad \tilde{u}_{O0}=A_1(Y)e^{ify}+A_2(Y)e^{-ify} \quad (15)$$

where $f^2=-N^2_\infty$. To avoid a secular term at the next order ($\tilde{u}_{O1}$) we require:

$$A'_1+\frac{A_1}{2Y}=0 \qquad \text{and} \qquad A'_2+\frac{A_2}{2Y}=0 \qquad \Rightarrow \qquad \tilde{u}_{O0}=\frac{1}{\sqrt{Y}}(A_1e^{ify}+A_2e^{-ify}). \quad (16)$$

Now this solution is singular at the origin, so to eliminate one of the two constants we need to solve for $\tilde{u}_O$ in an inner-outer region about $r=0$ where the $1/r$ terms become large. To do this we set $r=\delta x$ and expand our equations to leading order in δ. This gives:

$$N^2_\infty\xi\tilde{u}_{O0}-\xi\tilde{u}_{O0xx}-\frac{\xi}{x}\tilde{u}_{O0x}=0 \qquad \Rightarrow \qquad \tilde{u}_{O0}=AJ_0(fx). \quad (17)$$

For large x this solution can be approximated by the standard result:

$$\tilde{u}_{O0} \approx A\sqrt{\frac{2\delta}{f\pi Y}}\cos(fy - \frac{\pi}{4}) \tag{18}$$

This now has to match with our outer solution. This means that the Outer must be:

$$\tilde{u}_{O0} = \frac{\tilde{u}_{2\infty}}{\sqrt{Y}}\cos(fy - \frac{\pi}{4}) \qquad \text{and} \qquad A = \sqrt{\frac{f\pi}{2\delta}}\tilde{u}_{2\infty} \tag{19}$$

We can use a similar method to find the leading order terms of $\tilde{T}$, $\tilde{v}$ and $\tilde{p}$:

$$\tilde{T}_{O0} = \frac{\tilde{T}_{2\infty}}{\sqrt{Y}}\cos(f\sigma y - \frac{\pi}{4}) \tag{20a}$$

$$\tilde{v}_{O0} = \frac{\delta i(k-k^\star)\tilde{u}_{2\infty}}{f\sqrt{Y}}\sin(fy - \frac{\pi}{4}) - \frac{\delta f\xi(\gamma-1)\tilde{T}_{2\infty}}{\sigma\sqrt{Y}}\sin(f\sigma y - \frac{\pi}{4}) + \delta^2 C_1(Y) \tag{20b}$$

$$\tilde{p}_{O1} = \delta^2\xi^2 N_\infty^2(\gamma-1)\Big(2 + \frac{\mu_0^{B^*}}{\mu_0^*} - \frac{2}{3} - \frac{1}{Pr}\Big)\tilde{T}_{O0} + \delta^2 D_1(Y) \tag{20c}$$

To find the slowly varying terms of $\tilde{v}_O$ and $\tilde{p}_O$, we have to introduce a new slow-slow variable X such that $r = X/\delta + Y + \delta y$. We can then repeat the above method to second order and find that $C_1(r)$and $D_1(r)$ are the same Outer solutions, $\tilde{v}_{2O}$ and $\tilde{p}_{2O}$, as in the case $N_\infty^2 > 0$.

The constants $\tilde{u}_{2\infty}$ and $\tilde{T}_{2\infty}$ are both $\mathcal{O}(\varepsilon^2/\delta^2)$. This corresponds to an amplified acoustic streaming, stronger than the $\mathcal{O}(\varepsilon^2)$ acoustic streaming that would be expected, that is caused by the viscous boundary layer over the acoustic lining.

VI. Numerical Method

While asymptotic approximate solutions to equations (7,11,14) are possible (see, e.g. Refs. 1,14, here these equations are solved numerically using 4th order finite differences. The resulting $3N \times 3N$ banded matrix system of equations is solved using the LAPACK_ZGBSV routine. To solve for the first order nonlinear inner, the same matrix is used, now forced by terms nonlinear in the leading order quantities. The system of equations is solved from $y = 0$ to $y = Y$, where Y is large enough so that the mean flow terms are approximately there uniform flow values, and the extrapolation condition (8) is used as the boundary condition.

By way of comparison, we also produce weakly nonlinear solutions to the full Navier Stokes equations, without any of the asymptotic assumptions in δ and the matching needed above. The full Navier Stokes equations are expanded in ε, and a 4th order finite difference scheme is again used for the $\mathcal{O}(\varepsilon)$ and $\mathcal{O}(\varepsilon^2)$ equations thus obtained. In this case we get a $5N \times 5N$ banded matrix equation that is homogeneous in the leading order case and forced by leading order terms in the first order case. To accurately resolve the details in the boundary layer while still solving across the whole duct, stretched coordinates $\eta = \tanh(Sr)/\tanh(S)$ are used, where S is the stretching factor. This then concentrates the grid points about $r = 1$ so that the rapid variations there due to the thin boundary layer are properly resolved. For the results below a stretching factor of $S = 2.0$ is used. Before solving, the matrix is balanced so that the largest value in each row is 1; this ensures that the solution remains stable near the origin, where terms involving $1/r$ can become large.

VII. Results

Figure 4 shows plots of the mode shapes for both types of cross-interaction modes. The asymptotic solution can be seen to be in good agreement with the comparable result derived directly from the expansion in ε of the full Navier Stokes, calculated without assumptions about asymptotics and matching. Note that these solutions are calculated with $\tilde{p}_1 = 1$ at the wall, and only the real parts of the solutions are plotted here.

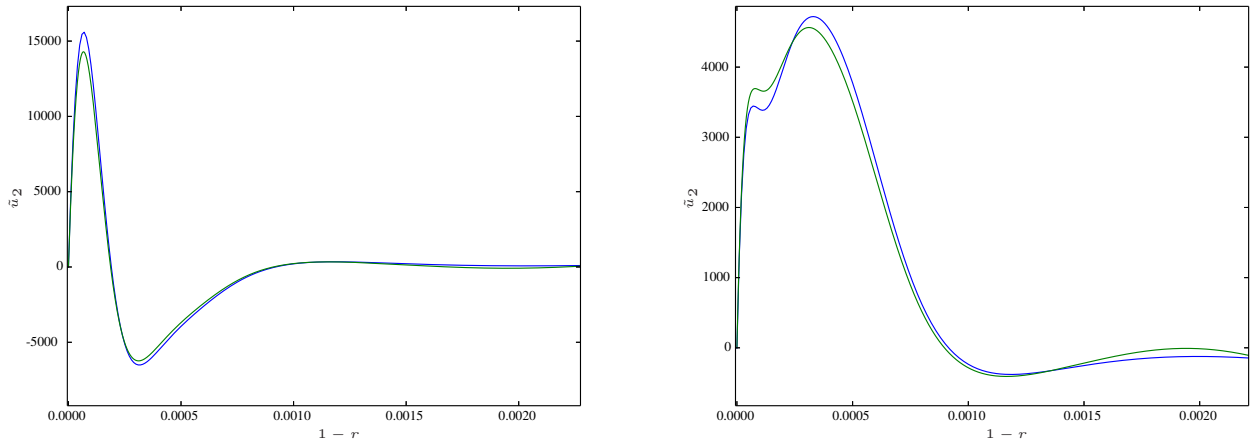

Figure 4: Inner solutions of $\tilde{u}_{2+}/\varepsilon^2$ (left) and $\tilde{u}_{2-}/\varepsilon^2$ (right) for $w_a = 5$, $k_a = 10$, $m_a = 10$, $w_b = 31 + 5i$, $k_b = 12$, $m_b = 12$ for asymptotics (blue) compared to expanded full Navier Stokes (green), with $\delta = 10^{-3}$, $M = 0.7$, Pr $= 0.7$ and $\xi = 1$

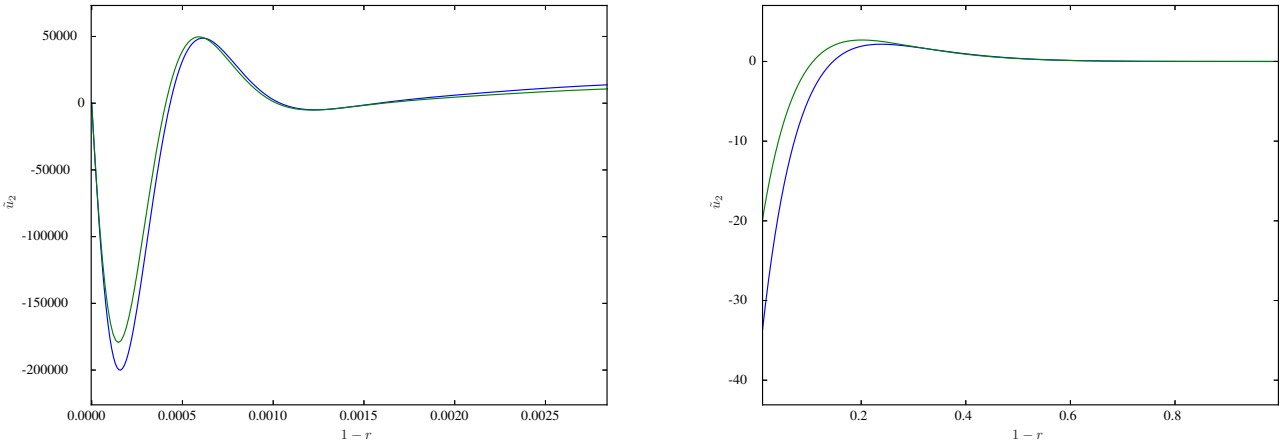

Figure 5: Inner (left) and outer (right) mode shapes of the double frequency mode $\tilde{u}_2/\varepsilon^2$, comparing the asymptotics (blue) to the first term from the expansion in ε of the full Navier Stokes (green). Parameters are $M = 0.7$, $\delta = 10^{-3}$, Pr $= 0.7$, $\xi = 1$, $\omega = 5$, $k = 5 + \mathrm{i}$ and $m = 2$

A typical mode shape of the double-frequency nonlinear mode is given in figure 5. The nonlinear asymptotic solution is shown to be in good agreement with be first term from the expansion in ε of the full Navier Stokes, giving confidence in the asymptotic method applied. Moreover, both solutions are localized within the boundary layer ($\delta = 10^{-3}$ in this case), confirming the prediction that the $\mathcal{O}(1/\delta)$ amplification within the boundary layer[1] does indeed trigger significantly more nonlinearity than would otherwise have been expected, but that, for the double frequency mode, it does not bleed out into the rest of the duct.

The comparable 'zero' frequency nonlinear mode, for the case upstream decaying case $N_\infty^2 > 0$, is plotted in figure 6. This shows a similar trend to 5, in that the predicted $\mathcal{O}(1/\delta)$ amplification within the boundary layer is seen, but does not bleed out into the rest of the duct; the acoustic streaming in the centre of the duct remains the classical magnitude of $\mathcal{O}(\varepsilon^2\delta^0)$.

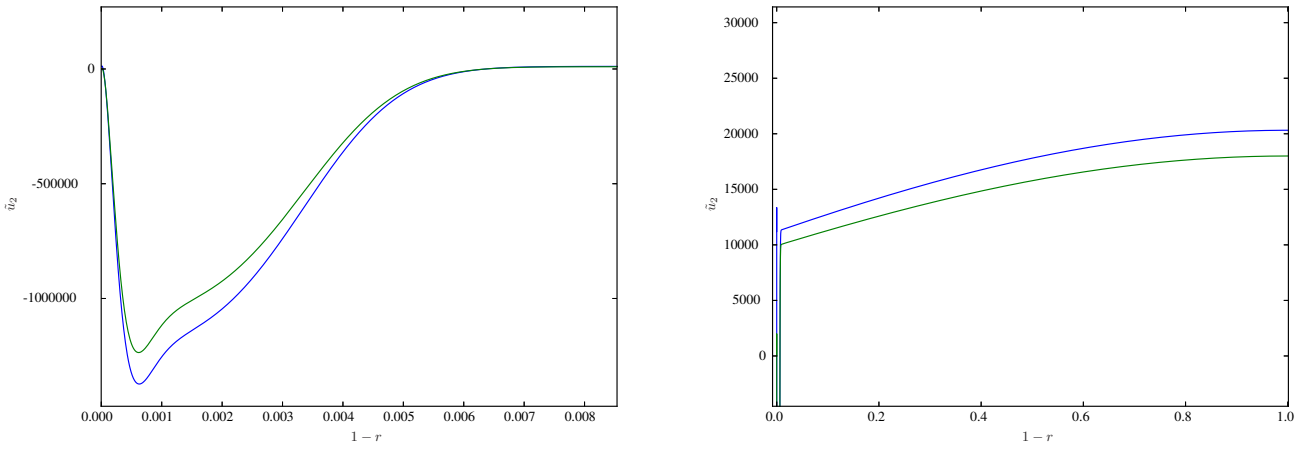

Figure 6: Inner (left) and outer (right) of 'zero' mode $\tilde{u}_2/\varepsilon^2$ for $\omega = 5$, $k = 5 + \mathrm{i}$ and $m = 2$ for asymptotics (blue) compared to the first term from the expansion in ε of the full Navier Stokes (green). Other parameters are $M = 0.7$, $\delta = 10^{-3}$, $\mathrm{Pr} = 0.7$ and $\xi = 1$

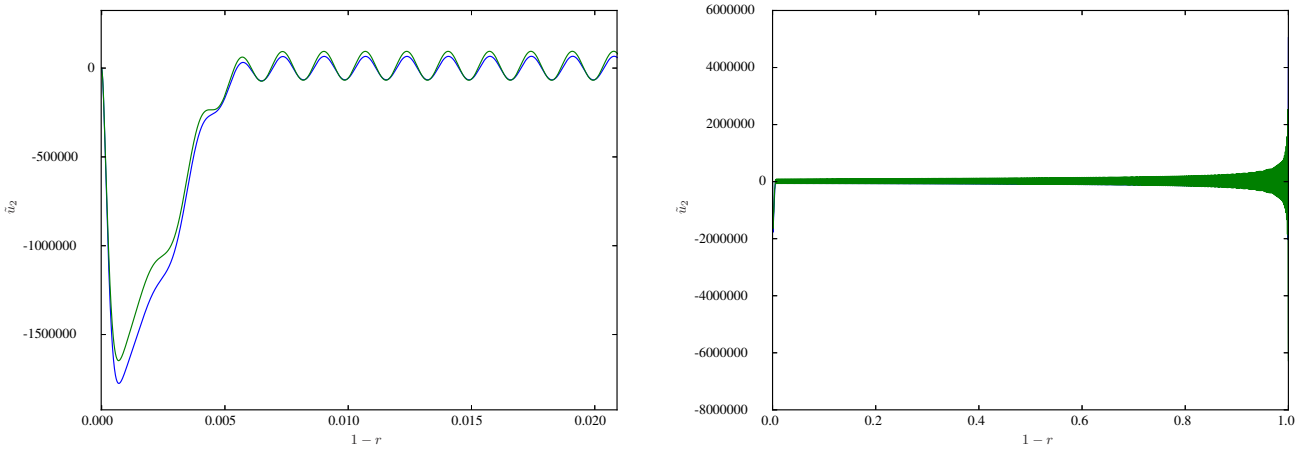

Figure 7: Inner (left) and outer (right) of 'zero' mode $\tilde{u}_2/\varepsilon^2$ for $\omega = 5$, $k = 5 - \mathrm{i}$ and $m = 2$ for asymptotics (blue) compared to the first term from the expansion in ε of the full Navier Stokes (green). Other parameters are $M = 0.7$, $\delta = 10^{-3}$, $\mathrm{Pr} = 0.7$ and $\xi = 1$

In contrast, however, figure 7 shows the mode-shapes in the case of a downstream decaying mode, for which $N_\infty^2 < 0$. The solution is seen to oscillate rapidly in r with a wavelength of order $\mathcal{O}(\delta)$. This amplified rapid oscillation does not decay away from the boundary layer and is present throughout the duct, with an amplitude of $\mathcal{O}(\varepsilon^2/\delta^2)$. This shows that, in this case, the amplification within the boundary layer by a factor of $1/\delta$ previously predicted[1] does indeed lead to significant nonlinearity beyond what would have been expected within the duct, and that this nonlinearity is not in this case confined to within the boundary layer but bleeds out into the rest of the duct.

Figure 8 shows the total sum of these effects, by plotting the overall perturbation to the streamwise velocity $\tilde{u}$ at different acoustic amplitudes. The effect of the nonlinear streaming is easily seen by the hairy appearance of the louder plot, although this nonlinear perturbation decays faster in the x direction than the damped acoustics, since the axial wavenumber has twice the decay rate of the linear acoustics.

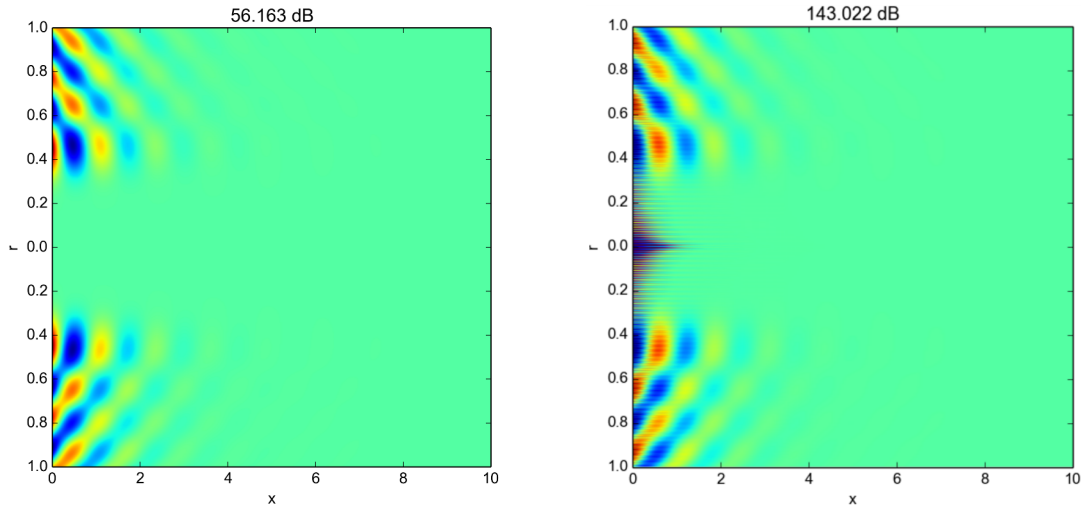

Figure 8: Plot of snapshots of the total perturbation for $k = 5 - i$, $\omega = 31$, $m = 10$ and $\delta = 10^{-3}$ for different initial amplitudes.

VIII. Conclusion

In this paper, we have investigated how the previously predicted[1] amplification of acoustics within a thin visco-thermal boundary layer over an acoustic lining leads to nonlinear effects becoming apparent at lower sound amplitudes than might have otherwise been predicted. It is emphasized that the nonlinearity presented here is nonlinearity within the fluid in the boundary layer, and is separate to the nonlinear behaviour of the actual boundary, such as the nonlinear behaviour of Helmholtz resonators near resonance[3]. The mechanism is that sound of amplitude ε enters the boundary layer of thickness δ and is amplified to order ε/δ. Nonlinear interactions then result in new acoustics with an amplitude of order ε^2/δ^2. These new acoustics have either double the frequency of the incoming sound, or 'zero' times the frequency, the latter corresponding to acoustic streaming. The double frequency amplified sound is localized to the boundary layer, but for downstream decaying sound the 'zero' frequency nonlinear modes bleed into the rest of the duct and show an ε^2/δ^2 amplitude throughout the duct. This is a factor of $1/\delta^2$ times the magnitude that would be created by ordinary nonlinear interactions within the duct itself.

Also derived here are equations governing the nonlinear interactions of two modes of differing frequencies. As for the self-interacting case, nonlinearity becomes important at lower amplitudes than expected due to the $1/\delta$ amplification within the boundary layer. Such interactions may well be important when two well-damped high azimuthal order spinning modes (for example, corresponding to the number of rotor and stator blades respectively) interact to produce a poorly-damped low azimuthal order nonlinear mode.

So far, this analysis has not been applied to investigate nonlinearity within surface modes[17,18]. Since surface modes are localized close to the boundary, and since one of them might be an instability which might lead to large amplitudes, investigating the impact of nonlinearity on such modes in combination with the $1/\delta$ amplification would prove interesting. For example, it may be that the nonlinearity enhances certain surface modes and restrains others.

The analysis presented here has assumed a thin boundary layer of width δ, and a small acoustic perturbation of amplitude ε, with $\varepsilon \ll \delta \ll 1$. In practice this is expected to be applicable to aircraft engines up to about 160dB, where nonlinear effects are expected to become important everywhere and not just confined to the boundaries. While the use of the asymptotics simplifies the governing equations, numerical solutions are still needed. In the linear case, other additional methods are used to derive approximate solutions and an effective impedance Z_{eff} that accounts for the behaviour within the boundary layer without having to numerically solve differential equations[1,13,14], and such techniques may well be applicable here.

Since these modes have only been identified mathematically, it would be interesting to look for their signature in existing experimental results, such as those of Aurégan[2], for example.

References

[1] Brambley, E. J., "Acoustic Implications of a Thin Viscous Boundary Layer over a Compliant Surface or Permeable Liner," *J. Fluid Mech.*, Vol. 678, 2011, pp. 348–378.

[2] Aurégan, Y. and Leroux, M., "Experimental Evidence of an Instability over an Impedance Wall in a Duct with Flow," *J. Sound Vib.*, Vol. 317, 2008, pp. 432–439.

[3] Singh, D. K. and Rienstra, S. W., "Non-linear Asymptotic Impedance Model for a Helmholtz Resonator Liner," *J. Sound Vib.*, Vol. 333, 2014, pp. 3536–3549.

[4] Myers, M. K., "On the Acoustic Boundary Condition in the Presence of Flow," *J. Sound Vib.*, Vol. 71, 1980, pp. 429–434.

[5] Aurégan, Y., Starobinski, R., and Pagneux, V., "Influence of Grazing Flow and Dissipation Effects on the Acoustic Boundary Conditions at a Lined Wall," *J. Acoust. Soc. Am.*, Vol. 109, 2001, pp. 59–64.

[6] Eversman, W. and Beckemeyer, R. J., "Transmission of Sound in Ducts with Thin Shear Layers — Convergence to the Uniform Flow Case," *J. Acoust. Soc. Am.*, Vol. 52, 1972, pp. 216–220.

[7] Tester, B. J., "The Propagation and Attenuation of sound in Lined Ducts containing Uniform or "Plug" Flow," *J. Sound Vib.*, Vol. 28, 1973, pp. 151–203.

[8] Brambley, E. J., "Fundamental Problems with the Model of Uniform Flow over Acoustic Linings," *J. Sound Vib.*, Vol. 322, 2009, pp. 1026–1037.

[9] Brambley, E. J., "A Well-Posed Boundary Condition for Acoustic Liners in Straight Ducts with Flow," *AIAA J.*, Vol. 49, No. 6, 2011, pp. 1272–1282.

[10] Renou, Y. and Aurégan, Y., "On a Modified Myers Boundary Condition to Match Lined Wall Impedance Deduced from Several Experimental Methods in Presence of a Grazing Flow," AIAA paper 2010-3945, 2010.

[11] Khamis, D. and Brambley, E. J., "The Effective Impedance of a Finite-Thickness Viscothermal Boundary Layer Over an Acoustic Lining," AIAA paper 2015-2229, 2015.

[12] Khamis, D. and Brambley, E. J., "Viscous Effects on the Attenuation of a Plane Wave by an Acoustic Lining in Shear Flow," *J. Acoust. Soc. Am.*, Vol. 141, No. 4, 2017, pp. 2408–2417.

[13] Khamis, D. and Brambley, E. J., "Viscous Effects on the Acoustics and Stability of a Shear Layer over an Impedance Wall," *J. Fluid Mech.*, Vol. 810, 2017, pp. 489–534.

[14] Khamis, D. and Brambley, E. J., "Acoustics in a two-deck viscothermal boundary layer over an impedance surface," *AIAA J.*, Vol. 55, No. 10, 2017, pp. 3328–3345.

[15] Landau, L. D. and Lifshitz, E. M., *Fluid Mechanics*, Elsevier, 2nd ed., 1987.

[16] Prangsma, G. J., Alberga, A. H., and Beenakker, J. J. M., "Ultrasonic Determination of the Volume Viscosity of N_2, CO, CH_4 and CD_4 between 77 and 300K," *Physica*, Vol. 64, 1973, pp. 278–288.

[17] Rienstra, S. W., "A Classification of Duct Modes based on Surface Waves," *Wave Motion*, Vol. 37, 2003, pp. 119–135.

[18] Brambley, E. J., "Surface Modes in Sheared Boundary Layers over Impedance Linings," *J. Sound Vib.*, Vol. 332, 2013, pp. 3750–3767.